



# Gaussian resolutions for equilibrium density matrices

Pavel Frantsuzov<sup>a,b</sup>, Arnold Neumaier<sup>c</sup>, Vladimir A. Mandelshtam<sup>a,\*</sup>

<sup>a</sup> Chemistry Department, University of California at Irvine, 516 Rowland Hall, Irvine, CA 92697-2025, USA

<sup>b</sup> Institute of Chemical Kinetics and Combustion RAS, Novosibirsk 630090, Russia

<sup>c</sup> Institut für Mathematik, Universität Wien, Strudlhofgasse 4, Wien A-1090, Austria

Received 27 June 2003; in final form 10 September 2003

Published online: 15 October 2003

## Abstract

The Gaussian wavepacket propagation method of Helling et al. [Chem. Phys. Lett. 122 (1985) 303] for the computation of equilibrium density matrices  $\hat{\rho}_T$  is revisited and modified. The variational principle applied to the ‘imaginary time’ Schrödinger equation provides the equations of motion for Gaussians in a resolution of  $\hat{\rho}_T$ , described by their width matrix, center and scale factor, all treated as dynamical variables. The method is computationally very inexpensive, has favorable scaling with the system size and, with the current implementation, is surprisingly accurate in a wide temperature range, even for cases involving quantum tunneling. Incorporation of symmetry constraints, such as reflection or particle statistics, is discussed as well.

© 2003 Published by Elsevier B.V.

## 1. Introduction

Computing the equilibrium quantum density matrix

$$\hat{\rho}_T := Z^{-1} e^{-\beta \hat{H}}, \quad Z := \text{Tr} e^{-\beta \hat{H}}, \quad (1)$$

in dependence of the inverse temperature  $\beta = 1/kT$ , or finding an equilibrium property of the type

$$\langle \hat{A} \rangle_T := \text{Tr} \hat{\rho}_T \hat{A}, \quad (2)$$

for some operator  $\hat{A}$ , is of great interest in statistical physics and molecular dynamics. The most accurate methods, based on a spectral resolution

$$\hat{\rho}_T = \sum_n e^{-\beta E_n} |n\rangle \langle n|,$$

are extremely expensive and limited to very few degrees of freedom. Methods based on solving the Bloch equation by explicit propagation of the density matrix [1,2] in ‘imaginary time’ ( $\beta$ ) have similar limitations. Commonly used practical, albeit still very expensive, strategies involve path integrals [3]. Alternative semiclassical approaches also exist (see, e.g., the recent Letter [4]), but they are either inaccurate or also expensive. In [5] Helling, Sawada and Metiu proposed a simple method for evaluating the equilibrium density

\* Corresponding author. Fax: +1-949-824-8571.

E-mail address: [mandelsh@uci.edu](mailto:mandelsh@uci.edu) (V.A. Mandelshtam).

URL: <http://www.mat.univie.ac.at/~neum>.

matrix. From now on we will refer to it as HSM. This method adapted the Gaussian wavepacket propagation techniques used previously to solve the real-time Schrödinger equation [6,7]. HSM reported results for 1D Morse and symmetric double-well potentials. Their general conclusion was that the method could give accurate results for sufficiently ‘heavy’ quantum particles or, equivalently, sufficiently high temperatures. In this Letter we modify their method. The present implementation shares the simplicity and efficiency of the HSM method, but is more accurate.

We also show how to incorporate certain symmetry constraints, such as reflection or particle statistics, while preserving the method’s simplicity and efficiency. The case of fermion statistics is especially important as the path-integral alternatives are very hard to use because of the so called ‘sign problem’. The corresponding applications as well as extensions to non-equilibrium problems will be discussed elsewhere.

## 2. Propagating Gaussian resolutions

Consider a  $N$ -body (or  $D = 3N$ -dimensional) quantum system with Hamiltonian

$$\hat{H} = \frac{1}{2} \hat{p}^T M^{-1} \hat{p} + U(x). \quad (3)$$

Here  $\hat{p}(x)$  define  $D$ -dimensional column vectors of momentum (coordinate) operators and  $M$  is the mass matrix. The potential function  $U(x)$  is assumed to be representable as a sum of terms, each being a product of a complex Gaussian times a polynomial. (With this assumption a commonly used plane wave representation of  $U(x)$  is covered.)

Given a grid  $q_n$  spanning the physically relevant region in configuration space we put

$$|q_{n,\tau}\rangle := e^{-\tau \hat{H}} |q_n\rangle, \quad (4)$$

with  $\langle x|q_n\rangle = \delta(x - q_n)$ . The resolution of identity can be approximated by

$$\hat{I} = \int d^D q |q\rangle \langle q| \approx \sum_n w_n |q_n\rangle \langle q_n|, \quad (5)$$

where the sum is over all the grid points and the  $w_n$  are quadrature weights defined by the inverse local density of  $q_n$ . (For large number of dimensions  $D$  a Monte Carlo procedure to generate  $q_n$  may be adopted.) Writing  $e^{-\beta \hat{H}} = e^{-\beta \hat{H}/2} \hat{I} e^{-\beta \hat{H}/2}$  and inserting Eq. (5), we obtain

$$Z \approx \sum w_n \langle q_{n,\beta/2} | q_{n,\beta/2} \rangle, \quad (6)$$

$$\hat{\rho}_T \approx Z^{-1} \sum w_n |q_{n,\beta/2}\rangle \langle q_{n,\beta/2}|. \quad (7)$$

To find  $|q_{n,\beta/2}\rangle$  we note that it is the solution of the initial-value problem

$$\frac{d}{d\tau} |q_{n,\tau}\rangle = -\hat{H} |q_{n,\tau}\rangle, \quad |q_{n,0}\rangle = |q_n\rangle. \quad (8)$$

We solve Eq. (8) approximately using the ansatz [5–9]

$$|q_{n,\tau}\rangle \approx |\lambda(\tau)\rangle, \quad (9)$$

with

$$\langle x | \lambda(\tau) \rangle = \exp \left\{ \gamma(\tau) - \frac{1}{2} [x - q(\tau)]^T G(\tau) [x - q(\tau)] \right\}. \quad (10)$$

This is a Gaussian with center  $q$ , a real vector, width matrix  $G$ , real symmetric and positive definite, and scale  $\gamma$ , a real constant, and  $\lambda := (G, q, \gamma)$ , a short-cut notation containing all the Gaussian parameters.

With this ansatz the maximum number of parameters corresponding to the use of full  $D \times D$  dimensional matrix  $G$  is  $(D+2)(D+1)/2$ . This number may possibly be reduced assuming weak coupling between certain degrees of freedom and setting the corresponding matrix elements of  $G$  to zero. The minimum number of  $2D+1$  parameters would correspond to using a diagonal width matrix  $G$ .

To solve for  $\lambda = \lambda(\tau)$  we follow the corresponding derivations [6–9] for the real and imaginary [5] time dynamics of a Gaussian wavepacket by utilizing the variational principle

$$\left[ \frac{\partial L}{\partial \lambda'} \right]_{\lambda'=\lambda} = 0, \quad (11)$$

with the Lagrangian

$$L = \left\langle \lambda'(\tau) \left| \frac{d}{d\tau} + \hat{H} \right| \lambda(\tau) \right\rangle. \quad (12)$$

Defining the two matrices

$$K = \langle \lambda' | \lambda \rangle, \quad H = \langle \lambda' | \hat{H} | \lambda \rangle, \quad (13)$$

Eq. (11) can be rewritten as

$$\left[ \frac{\partial^2 K}{\partial \lambda \partial \lambda'} \dot{\lambda} + \frac{\partial H}{\partial \lambda'} \right]_{\lambda'=\lambda} = 0, \quad (14)$$

thus providing the equations of motion for the Gaussian parameters  $\lambda = \lambda(\tau)$ . Note that HSM [5] utilized a different variational principle, which may or may not lead to different results.

The use of the Gaussian wavepackets and the assumed form of the Hamiltonian (3) allows one to evaluate the corresponding matrix elements and their derivatives in Eq. (14) analytically. (Efficient numerical expressions will be published elsewhere, but see [7,9].) Note that the commonly used linearization of the potential [6] reduces the complexity of the matrix elements evaluation, but also the accuracy (see, e.g., [5]), and is not used here.

The delta function in the initial condition of Eq. (8) can be considered as a limit of the Gaussian (10) with infinite  $G$ . To avoid the singularities at  $\tau = 0$  we start instead at some small  $\tau_0$  where we approximate  $|q_{n,\tau_0}\rangle$  by a Gaussian that has finite width

$$\begin{aligned} \langle x | \lambda(\tau_0) \rangle &\approx \sqrt{\frac{\det M}{(2\pi\tau_0)^d}} \times \exp \left[ -\frac{1}{2\tau_0} (x - q_n)^T \right. \\ &\quad \left. \times M (x - q_n) - U(q_n)\tau_0 \right]. \end{aligned} \quad (15)$$

To solve Eq. (14), we use the implicit integrator DASSL [10], which has an error control and can be applied directly to Eq. (14). (Probably, a standard numerical integrator could be utilized, if Eq. (14) is explicitly solved for  $\dot{\lambda}$ .) We did not encounter any special numerical difficulties, except in the cases when the Gaussian width was too small. Note that  $\beta$  is small at large temperature  $kT = 1/\beta$ , and only a few integration steps are needed. As  $T$  decreases, the integration time becomes larger, and the variational approximation by Gaussians may become poorer.

Given (9), we can rewrite (7) as

$$\hat{\rho}_T \approx Z^{-1} \sum w_n |\lambda_n(\beta/2)\rangle \langle \lambda_n(\beta/2)|, \quad (16)$$

where

$$Z \approx \sum w_n \langle \lambda_n(\beta/2) | \lambda_n(\beta/2) \rangle, \quad (17)$$

and get for expectations

$$\langle A \rangle_T \approx Z^{-1} \sum w_n \langle \lambda_n(\beta/2) | \hat{A} | \lambda_n(\beta/2) \rangle. \quad (18)$$

The evaluation of  $\langle A \rangle$  requires the computation of many matrix elements of  $\hat{A}$  between new Gaussian wavepackets for every value of  $T$ . This can be done analytically if  $A$  is polynomial in  $p, x$  or the product of a polynomial and a complex Gaussian.

The most important difference of the present implementation with the method of HSM is in Eq. (16), which is new. HSM derived equations to evaluate the  $x'$ -column of the unnormalized density matrix

$$\langle x | e^{-\beta H} | x' \rangle \approx \langle x | \lambda_{x'}(\beta) \rangle, \quad (19)$$

where  $|\lambda_{x'}(\beta)\rangle$  is a Gaussian propagated using differential equations similar to Eq. (14) with the initial Gaussian centered at  $x'$  using a form similar to that in Eq. (15). Note the absence of the partition function  $Z_T$  in Eq. (19). Moreover, Eq. (19) is non-symmetric with respect to  $x$  and  $x'$ . This unphysical feature implies that at sufficiently low temperatures observables such as the density  $\langle x | \hat{\rho}_T | x \rangle$  may have artifacts, e.g., discontinuities or other spurious effects. Such artifacts do not occur in the present implementation. HSM mentioned the possibility of using a symmetric form, but did not pursue it.

### 3. Taking into account symmetry

Very often the system in question has symmetries, that is, the corresponding time-dependent Schrödinger equation conserves certain symmetries. To show how to utilize this, we consider the example of reflection symmetry,  $\hat{S}\psi(x) = \psi(-x)$ , and assume that

$$|q_{n,\tau}^\pm\rangle = \frac{1}{\sqrt{2}} (|q_{n,\tau}\rangle \pm \hat{S}|q_{n,\tau}\rangle), \quad (20)$$

is a solution of Eq. (8) at any  $\tau$ . Rewriting the resolution of identity,

$$\hat{I} \approx \sum_n w_n (|q_n^+\rangle \langle q_n^+| + |q_n^-\rangle \langle q_n^-|), \quad (21)$$

we obtain

$$\begin{aligned} Z &\approx \sum w_n (\langle q_{n,\beta/2}^+ | q_{n,\beta/2}^+ \rangle + \langle q_{n,\beta/2}^- | q_{n,\beta/2}^- \rangle), \\ \hat{\rho} &\approx Z^{-1} \sum w_n (|q_{n,\beta/2}^+ \rangle \langle q_{n,\beta/2}^+| + |q_{n,\beta/2}^- \rangle \langle q_{n,\beta/2}^-|), \\ \langle A \rangle &\approx Z^{-1} \sum w_n (\langle q_{n,\beta/2}^+ | \hat{A} | q_{n,\beta/2}^+ \rangle + \langle q_{n,\beta/2}^- | \hat{A} | q_{n,\beta/2}^- \rangle). \end{aligned} \quad (22)$$

To approximate the solutions  $|q_{n,\tau}^\pm\rangle$  we can replace the Gaussian in Eq. (9) by the symmetrized Gaussian

$$|\lambda_\pm\rangle = \frac{1}{\sqrt{2}} (|\lambda\rangle \pm \hat{S}|\lambda\rangle), \quad (23)$$

where

$$\hat{S}|G(\tau), q(\tau), \gamma(\tau)\rangle = |G(\tau), -q(\tau), \gamma(\tau)\rangle.$$

Therefore, the matrix elements needed in Eq. (14) can be evaluated by taking the appropriate linear combinations of matrix elements between single Gaussians.

#### 4. Bose and Fermi statistics

Another important case of symmetry corresponds to the Bose or Fermi statistics. For a system of  $N$  indistinguishable particles in configuration space defined by the coordinates

$$x = (x_1, \dots, x_N)^T,$$

we should symmetrize or antisymmetrize the wavepackets according to the particle statistics. Let  $\alpha = (\alpha_1, \dots, \alpha_N)$  define a permutation of particle indices, and denote by  $P_\alpha$  the permutation matrix with

$$P_\alpha x = (x_{\alpha_1}, \dots, x_{\alpha_N})^T.$$

A symmetrized wavepacket  $|\lambda_\pm\rangle$  can be defined by

$$\langle x | \lambda_\pm \rangle = \sum_\alpha \text{sign}_\pm(\alpha) \langle P_\alpha x | \lambda \rangle. \quad (24)$$

Here boson statistics has  $\text{sign}_-(\alpha) = 1$ ; in the case of fermion statistics,  $\text{sign}_+(\alpha) = 1$  for even permutations and  $\text{sign}_+(\alpha) = -1$  for odd permutations. The equations of motion (14) have the same general form. Since Eq. (24) implies

$$|\lambda_\pm\rangle = \sum_\alpha \text{sign}_\pm(\alpha) P_\alpha^* |\lambda\rangle,$$

and one easily verifies

$$P_\alpha^* |G, q, \gamma\rangle = |P_\alpha^* G P_\alpha, P_\alpha^* q, \gamma\rangle,$$

here again, matrix elements with symmetrized Gaussians  $|\lambda_\pm\rangle$  are simple linear combinations of suitable matrix elements with unsymmetrized Gaussians. Similar considerations apply to multi-particle systems with few indistinguishable particles, where the sum (24) has only a few terms and the calculations remain feasible.

### 5. Numerical examples

#### 5.1. 1D single-well problem

We first apply the method to a 1D problem of [4] with potential  $U(x) = \frac{1}{2}x^2 + 0.1x^4$  to compute the mean square displacement  $\langle x^2 \rangle - \langle x \rangle^2$  as a function of temperature  $T$ . A grid of 10 equidistant points was taken in the interval  $-5 < q_n < 5$ . (Here and in all the following examples the reported results fully converged with respect to the grid size.) Each of the 10 Gaussians was then propagated by Eq. (14) starting with  $\tau_0 = 0.01$  up to  $\tau = 50$ . The result obtained by the present method is hardly distinguishable from the converged quantum calculation using diagonalization of the Hamiltonian in a large basis. In Fig. 1 these results are also compared to

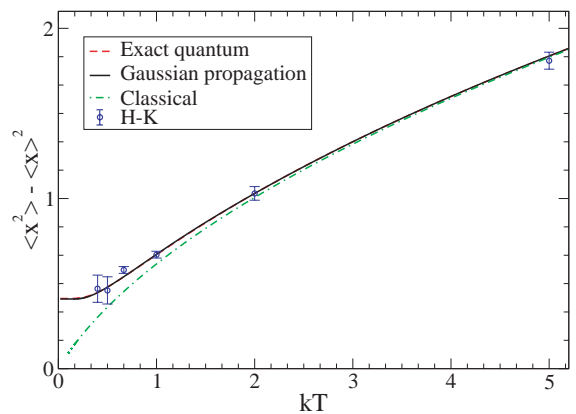


Fig. 1. Mean square displacement computed by four different methods for 1D single well potential  $U(x) = \frac{1}{2}x^2 + 0.1x^4$ . The semiclassical result labeled by 'H-K' is taken from [1]. The difference between the present and exact quantum result is not seen in the graph.

the classical Boltzmann average and to the semi-classical calculation using the Herman–Kluk propagator [4]. Note that in the latter case a much more expensive Monte Carlo method was used with  $10^5$  classical trajectories, still resulting in relatively big statistical errors.

We note that a similar high accuracy was achieved for a 2D single well problem (not shown here).

### 5.2. 1D symmetric double-well problem

Here the method was applied to a problem with the potential  $U(x) = 4 - 4x^2 + x^4$ . Now a grid of 14 points with  $-3 < q_n < 3$  was used. The corresponding results using both the unsymmetrized and symmetrized Gaussians are shown in Fig. 2. The agreement between the exact result (fully converged diagonalization of  $\hat{H}$  in a large basis) and that computed by the present method is unexpectedly excellent even at quite low temperatures, well below the potential barrier. For the unsymmetrized case a significant deviation from the exact (and symmetrized) result occurs only at low temperatures where the small tunneling splitting causes the quantum observables change rapidly with  $T$ .

In Fig. 3 we show the density profile for the same system computed using the same set of 14 symmetrized Gaussians at  $kT = 0.5$  together with the exact quantum and classical results.

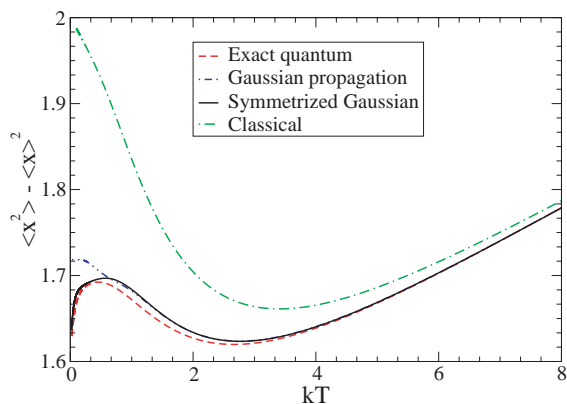


Fig. 2. The mean square displacement for the symmetric double-well potential  $U(x) = 4 - 4x^2 + x^4$  computed by four different methods.

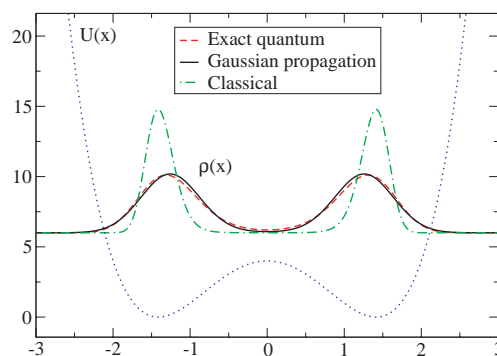


Fig. 3. The density  $\rho(x) = \langle x | \hat{\rho} | x \rangle$  at  $kT = 0.5$  computed by three different methods for the symmetric double-well potential  $U(x)$  as in Fig. 2.

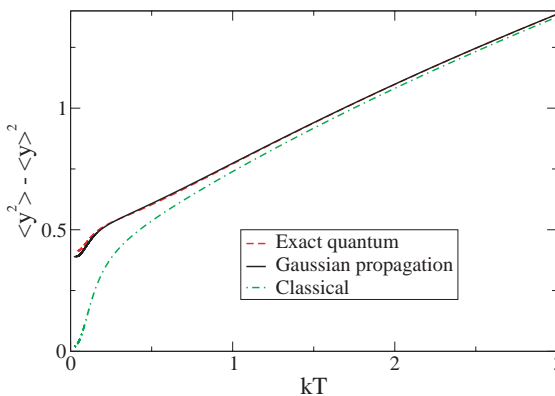
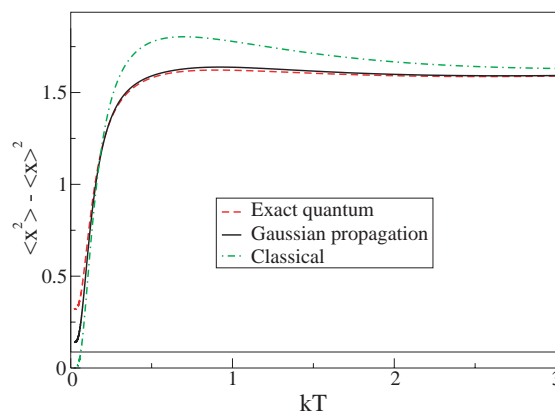


Fig. 4. The mean square displacements computed by three different methods for the asymmetric 2D double-well potential  $U(x, y) = (x^2 - 2)^2 + 0.1x + 0.5(y - 0.5x)^2 + 0.1y^4$ .

### 5.3. 2D asymmetric double-well problem

To further demonstrate the method we apply it to a 2D problem with asymmetric double-well potential  $U(x,y) = (x^2 - 2)^2 + 0.1x + 0.5(y - 0.5x)^2 + 0.1y^4$ . An equidistant  $16 \times 16$  grid  $q_n$  in a square box  $[-4; 4] \times [-4; 4]$  was used. The results for the mean square displacements shown in Fig. 4 are again surprisingly accurate, except for very low temperatures.

### Acknowledgements

We are grateful to Horia Metiu for useful remarks. V.A.M. acknowledges the NSF support, grant CHE-0108823. He is an Alfred P. Sloan research fellow.

### References

- [1] D. Thirumalai, E.J. Bruskin, B.J. Berne, J. Chem. Phys. 79 (1983) 5063.
- [2] B. Hellsing, A. Nitzan, H. Metiu, Chem. Phys. Lett. 123 (1986) 523.
- [3] R.P. Feynman, A.R. Hibbs, Quantum Mechanics and Path Integrals, McGraw-Hill, New York, 1965.
- [4] N. Makri, W.H. Miller, J. Chem. Phys. 116 (2002) 9207.
- [5] B. Hellsing, S. Sawada, H. Metiu, Chem. Phys. Lett. 122 (1985) 303.
- [6] E.J. Heller, J. Chem. Phys. 62 (1975) 1544.
- [7] A.I. Sawada, R.H. Heather, B. Jackson, H. Metiu, J. Chem. Phys. 83 (1985) 3009.
- [8] R.D. Coalson, M. Karplus, J. Chem. Phys. 93 (1990) 3919.
- [9] A.K. Pattanayak, W.C. Schieve, Phys. Rev. E 50 (1994) 3601.
- [10] L.R. Petzold, in: R.S. Stepleman et al. (Eds.), Scientific Computing, North-Holland, Amsterdam, 1983, p. 65.